J Appl Physiol
91: 2720–2729, 2001.

On the likelihood of decompression sickness during H_2 biochemical decompression in pigs

ANDREAS FAHLMAN,[1] PETER TIKUISIS,[2] JEFFREY F. HIMM,[1]
PAUL K. WEATHERSBY,[1] AND SUSAN R. KAYAR[1]
[1]*Environmental Physiology Department, Naval Medical Research Center, Silver Spring, Maryland 20910-7500; and* [2]*Defence and Civil Institute of Environmental Medicine, Toronto, Ontario, Canada M3M 3B9*

Received 30 October 2000; accepted in final form 23 August 2001

Fahlman, Andreas, Peter Tikuisis, Jeffrey F. Himm, Paul K. Weathersby, and Susan R. Kayar. On the likelihood of decompression sickness during H_2 biochemical decompression in pigs. *J Appl Physiol* 91: 2720–2729, 2001.—A probabilistic model was used to predict decompression sickness (DCS) outcome in pigs during exposures to hyperbaric H_2 to quantify the effects of H_2 biochemical decompression, a process in which metabolism of H_2 by intestinal microbes facilitates decompression. The data set included 109 exposures to 22–26 atm, ca. 88% H_2, 9% He, 2% O_2, 1% N_2, for 0.5–24 h. Single exponential kinetics described the tissue partial pressures (Ptis) of H_2 and He at time t: Ptis = $\int (\text{Pamb} - \text{Ptis}) \cdot \tau^{-1}\, dt$, where Pamb is ambient pressure and τ is a time constant. The probability of DCS [P(DCS)] was predicted from the risk function: $P(\text{DCS}) = 1 - e^{-r}$, where $r = \int (\text{Ptis}_{H_2} + \text{Ptis}_{He} - \text{Thr} - \text{Pamb}) \cdot \text{Pamb}^{-1}\, dt$, and Thr is a threshold parameter. Inclusion of a parameter (A) to estimate the effect of H_2 metabolism on P(DCS): $\text{Ptis}_{H_2} = \int (\text{Pamb} - A - \text{Ptis}_{H_2}) \cdot \tau^{-1}\, dt$, significantly improved the prediction of P(DCS). Thus lower P(DCS) was predicted by microbial H_2 metabolism during H_2 biochemical decompression.

probabilistic modeling; *Sus scrofa*; hydrogen diving; H_2 metabolism; *Methanobrevibacter smithii*

MODELING OF DECOMPRESSION SICKNESS (DCS) risk has been impeded by the inability to identify correlated physiological variables. Some studies have tried to find a correlation between DCS risk and variables such as body temperature, body weight, exercise, gender, adiposity, age, serum cholesterol, sensitivity to complement activation, Doppler bubble grades, and patent foramen ovale (4, 12, 16, 23, 28). However, where some studies have found a correlation, others refute those results (5, 8, 16). The only physiological variable that has been undisputedly correlated with DCS risk in rats is body weight (20). Because reliable physiological correlates are lacking, researchers have used a variety of models based solely on the physical history of the compression and decompression sequence to find variables that can predict the probability of DCS (26, 31–34).

The DCS risk assessment used in this study builds on previously published models used in DCS research (26, 31, 33, 34). The goal is to estimate the beneficial effects on DCS risk of the active removal of tissue H_2 by injecting H_2-metabolizing microbes into the intestines of pigs during simulated H_2 dives and to suggest a physiological mechanism for the process called H_2 biochemical decompression (19). The metabolism of H_2 in the intestine is readily followed by measuring the release of CH_4, the metabolic end product of the microbial metabolism (21)

$$4H_2 + CO_2 \rightarrow 2H_2O + CH_4 \qquad (1)$$

The model presented here differs from earlier models of DCS (26, 31, 33, 34) in that a parameter for the microbial metabolism of H_2 is included. In constructing this model, the microbial metabolism of H_2 was considered to have a direct physiological effect by influencing the gas kinetics. The measure of H_2 metabolism was based on either the total microbial activity injected into the animals (Inj), or as the CH_4 release rate ($\dot{V}_{CH_4}$) from individual animals, assuming that there is a direct correlation between the H_2 metabolized inside the intestines and the release of CH_4 from the intact animal (*Eq. 1*). This model was used to predict the advantage of biochemical decompression for hyperbaric H_2 exposures in general and thus offers a predictive advantage over the descriptive logistic regression model of biochemical decompression that was derived earlier (10, 18).

As a result, this study used a measured physiological variable, namely the rate of removal of H_2 by the metabolism of intestinal microbes, together with the physical history of the hyperbaric exposure to predict the DCS incidence after a hyperbaric exposure to H_2.

METHODS

Data Set and Case Descriptions

The data used in this study were taken from animal experiments previously reviewed and approved and have

Address for reprint requests and other correspondence: S. R. Kayar, Environmental Physiology Dept., Naval Medical Research Center, 503 Robert Grant Ave., Silver Spring, MD 20910-7500.

The costs of publication of this article were defrayed in part by the payment of page charges. The article must therefore be hereby marked "*advertisement*" in accordance with 18 U.S.C. Section 1734 solely to indicate this fact.

been reported in detail elsewhere (11, 18). A brief explanation of the experimental procedure will be provided here.

Pigs (*Sus scrofa*, 17–23 kg) were used for all experiments. The pigs were housed before experiments in an accredited animal care facility and had ad libitum access to water. The pigs were fed once daily with laboratory animal chow (Harlan Teklad, Madison, WI; 2% by body wt). All procedures were approved by an Animal Care and Use Committee. The experiments reported here were conducted according to the principles presented in the *Guide for the Care and Use of Laboratory Animals* (National Research Council, 1996).

The data set contains 109 well-documented hyperbaric exposures, with 53 severe DCS cases (Table 1). All animals were juvenile male Yorkshire pigs, either castrated ($n = 98$) or noncastrated ($n = 11$). There was no difference in DCS incidence between the castrated and noncastrated animals (logistic regression analysis, $P > 0.3$). Consequently, these two groups were pooled for all subsequent analyses.

The animals were divided into three groups: untreated control (UC, $n = 69$, mean body wt 19.6 ± 1.4 kg), surgical control (SC, $n = 11$, mean body wt 19.6 ± 1.6 kg), and treated ($n = 29$, mean body wt 19.5 ± 1.3 kg). Treated animals had H_2-metabolizing microbes injected into the large intestine (mean 0.92 ± 0.49 mmol CH_4/min, range 0.20–2.20 mmol CH_4/min), a procedure requiring major surgery. This surgical procedure and the culturing of *Methanobrevibacter smithii* are similar to prior work in rats (19) and have been described elsewhere (18). In the SC group, animals received intestinal injections of saline bubbled with CO_2 to deoxygenate it. The SC group has been described in detail along with the surgical procedure (18). Because DCS incidence was indistinguishable between the SC and UC groups ($P > 0.29$, Fisher exact test), the two groups were pooled and will be referred to as control animals (C = UC + SC, $n = 80$).

The experiments were carried out over a period of 30 mo (May 1997–Dec 1999) and include a variety of different pressurization and depressurization sequences (Table 1). The hyperbaric H_2 exposures were performed in a dry chamber (WSF Industries, Buffalo, NY) of 5,600-liter volume at 1 atm. Each animal was subjected to only one hyperbaric exposure. The chamber was controlled by a computer that stored the ambient pressure (Pamb, atm), chamber temperature (°C), O_2 concentration (%), and elapsed time (min). A gas chromatograph (Hewlett-Packard 5890A, Series II, Wilmington, DE) measured the chamber gases O_2, H_2, He, N_2, and CH_4 every 12 min.

Each hyperbaric exposure commenced with a pressurization of the chamber with He to 11 atm, followed by a flush of the chamber with H_2 until the H_2 concentration was over 60%. The initial pressurization with He was necessary as a safety measure to prevent an explosive mixture of H_2 and O_2 in the chamber, as described in detail elsewhere (18–20). Pressurization then continued with H_2, with addition of O_2 as needed to maintain normoxia (0.2–0.4 atm O_2). Maximum pressure of the exposures ranged from 22 to 26 atm (absolute pressure; 2.23–2.63 MPa; 700–825 feet of seawater pressure equivalent; Table 1). Final gas composition in the chamber at maximal pressure was roughly 88% H_2, 9% He, 2% O_2, and 1% N_2 for exposures lasting 3 h, with more H_2 and less He and N_2 present in the chamber over time. Chamber concentrations of CH_4 ranged from <1 ppm to 8 ppm after 3 h, and up to 40 ppm after 24 h.

The start of the decompression (*time 0*) was set as the time that animals were last definitely free of DCS signs (T_1). The chamber was decompressed at 0.45–1.8 atm/min to 11 atm while each animal was observed closely. Decompression could not continue past 11 atm because of the need for a normoxic environment and safe handling of H_2 and O_2 mixtures as described earlier (18–20). On arrival at 11 atm, the animal was made to walk on a treadmill inside the chamber at 5-min intervals for up to 1 h (67–90 min, Tend) or until the animal was declared to have DCS (T_2) (18).

Most animals displayed violaceous macular lesions with or without pruritus. On the basis of previous descriptions in the literature, these lesions resembled skin DCS (6, 9). However, skin DCS alone was not considered a DCS case for the purpose of this study. Severe DCS symptoms were of two types: cardiopulmonary or neurological (3, 6, 9). Severe symptoms of DCS included walking difficulties, fore- and/or hindlimb paralysis, falling, seizures, labored breathing, and convulsions. Every diagnosis of DCS was determined by a consensus of at least three observers who discussed their diagnosis as the events occurred. The observers were not blind to the treatments or dive profiles, resulting in the possibility of biased diagnosis. However, the rigorous compression and decompression sequences used throughout this

Table 1. *Experimental protocols*

Treatment Group	Inert Gas	Weight, kg	P, atm	*n*	DR, atm/min	Time, min	Inj, mmol CH_4/min	$\dot{V}_{CH_4}$, mmol CH_4/min	Outcome, % DCS
C	H_2/He	19.3 ± 1.1	22	13	0.45	180	0	0.04 ± 0.03	31
C	H_2/He	19.6 ± 1.5	24	9	0.45	180	0	0.03 ± 0.03	33
C	H_2/He	18.8 ± 1.3	26	7	0.45	180	0	0.04 ± 0.03	0
C	H_2/He	19.8 ± 1.5	24	20	0.9	180	0	0.03 ± 0.02	80
T	H_2/He	18.9 ± 1.0	24	18	0.9	180	0.98 ± 0.53	0.09 ± 0.03	39
C	H_2/He	20.6 ± 0.7	24	8	1.8	180	0	0.04 ± 0.03	100
T	H_2/He	21.2 ± 0.6	24	2	1.8	180	0.89 ± 0.49	0.10 ± 0.01	100
C	H_2/He	19.0 ± 1.1	24	8	0.9	150	0	0.04 ± 0.04	37
T	H_2/He	19.2 ± 1.2	24	5	0.9	150	0.91 ± 0.41	0.10 ± 0.03	40
C	H_2/He	20.9 ± 0.8	24	5	0.9	120	0	0.08 ± 0.04	80
C	H_2/He	19.0 ± 1.1	24	9	0.9	30	0	0.04 ± 0.02	22
C	H_2/He	21.4	24	1	0.9	1,100	0	0.02	100
T	H_2/He	20.6 ± 0.9	24	3	0.9	>1,100	0.78 ± 0.47	0.24 ± 0.04	33
T	He	20.7	24	1	0.9	180	0.24	0.02	0

Values are means ± SD. Group type [control (C) or treatment (T)], primary components of the gas mixture (Inert Gas), mean body weight of pigs, maximal ambient absolute pressure (P), number of animals in each group (*n*), decompression rate (DR), time held at maximum pressure (Time), mean total microbial activity injected (Inj), mean CH_4 release rate ($\dot{V}_{CH_4}$), and decompression sickness (DCS) outcome in each group. The groups are untreated and surgical control animals (C), and animals treated with H_2-metabolizing microbes injected into the intestine (T).

study caused signs of DCS that were in most cases severe enough to leave no ambiguity. In the rare event that the observers did not agree, a detailed description or a viewing of a video recording of the animal was given to a neurologist or diving medical officer to evaluate and pass final judgment.

DCS Risk Assessment Modeling

A model of the probability of DCS [*P*(DCS)] was defined, using the method of maximum likelihood to search for the best fitting parameters (7, 31). Experience has shown that elevated pressure, longer exposure to elevated pressure, and increasing decompression rate all increase the risk of DCS (14, 34). However, the occurrence is seldom either a certainty or zero for any hyperbaric exposure (34). Therefore, researchers have used probabilistic models to predict the *P*(DCS) in dives with varying compression and decompression profiles (31, 33, 34). In previous models, the outcome data for each hyperbaric exposure were used to estimate the model parameters. As a result, the parameters are a mathematical composition and have only limited physiological value (2).

The probabilistic models used previously, unlike most logistic regressions, were constructed to be well behaved in the sense that the *P*(DCS) was predicted to be 0 when no pressure reduction occurred and increased with increasing pressure reduction (34).

The probability of having DCS symptoms at a time t, after a hyperbaric exposure, is defined as

$$P(\text{DCS}) = 1.0 - \exp\left(-\int_0^T r\,dt\right) \quad (2)$$

whereas freedom of symptoms until time t is defined as

$$P(\text{no DCS}) = 1.0 - P(\text{DCS}) = \exp\left(-\int_0^T r\,dt\right) \quad (3)$$

where r is the instantaneous risk (7), and $r \geq 0$. The r depends on the theory used to describe the mechanism of DCS and can be one of several measures integrated over the dive and postdive period.

The probability of developing DCS for a particular hyperbaric exposure is defined as the integrated r over the exposure period through the end of the postdecompression observation period (Tend). Consequently, if DCS was observed, the following formula was used

$$P(\text{DCS}) = \left[\exp\left(-\int_0^{T_1} r\,dt\right)\right]\left[1.0 - \exp\left(-\int_{T_1}^{T_2} r\,dt\right)\right] \quad (4)$$

This is the product of the probability of DCS not occurring in the interval [0–T_1] and the probability of DCS occurring in the interval [T_1–T_2] (26, 34). T_1 is defined as the last time when the diver was definitely free of DCS symptoms, and T_2 the time the diver was declared to have definite signs of DCS (26, 34). For an animal with no DCS, *Eq. 2* is used to estimate the *P*(DCS) with the upper limit for integration at the end of the postdecompression observation period (Tend). For an animal displaying DCS, *Eq. 4* is used and the integration is performed until the time the animal definitely shows signs of DCS (T_2).

The choice of T_1 can be made in various ways, as detailed elsewhere (34). Because of subjective aspects inherent in diagnosing DCS, T_1 is set to the start of the decompression for this study. This approach is conservative and may result in some loss of temporal information. However, because T_1 is difficult to determine in some cases, this approach seems warranted.

Model Variations

Two models were tested, both describing r from a single tissue. One model used the speculation that the maximum r develops rapidly after a decompression step after which it decreases immediately as Pamb > Ptis (Immediate model, *Eq. 5*, Fig. 1*A*). The second model (Delayed model, *Eq. 6*, Fig. 1*B*) used the hypothesis that r increases more slowly to a maximum value, after which it decreases slowly.

It is widely accepted that the presence of gas bubbles in tissues leads to DCS (14). If one believes that the presence of bubbles triggers the symptoms, it may be most appropriate to use a risk function in which the greatest r occurs immediately after a decompression step (34). Alternatively, if one prefers the theory that DCS develops after the bubbles have

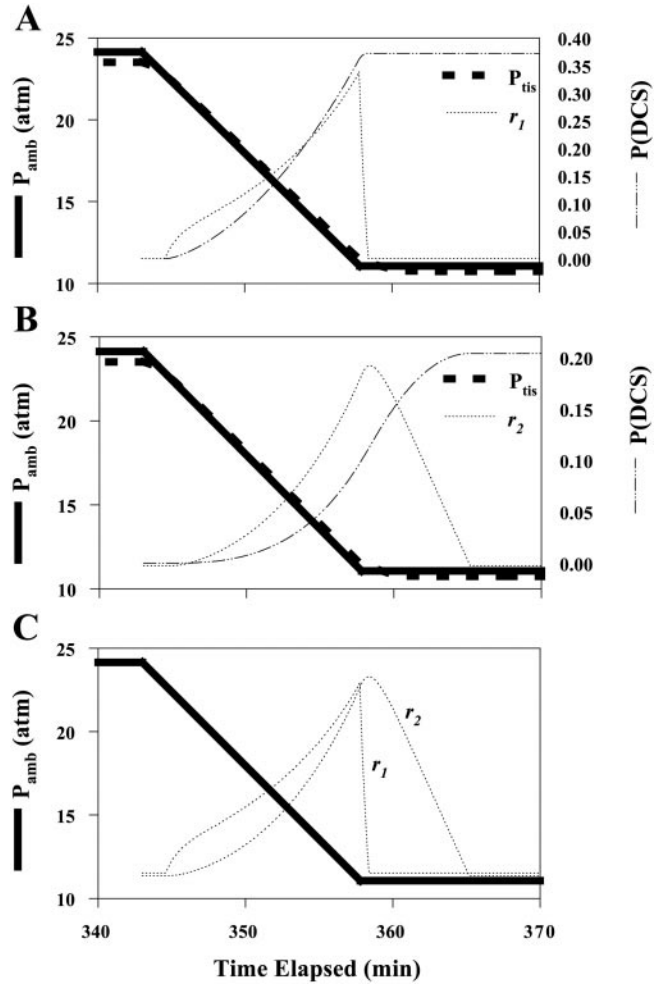

Fig. 1. Model behavior showing the ambient pressure (Pamb), estimated tissue tension for H_2 and He (Ptis), the probability of decompression sickness [DCS; *P*(DCS)], the instantaneous risk (r_1, *Eq. 5*) for the Immediate (*A*) model, and the relative supersaturation (r_2, *Eq. 6*) for the Delayed (*B*) model using a time constant (τ) and a scale factor (G) for a sample dive to 24 atm. The Pamb, the r_1, and the r_2 for both models (*C*) are displayed to show the delayed maximum for the r_2 compared with r_1. Constant pressure was maintained for 3 h followed by decompression at 0.9 atm/min to 11 atm. The Immediate model (*A*) used $\tau = 0.80$ and $G = 2.23$ whereas the Delayed model (*B*) used $\tau = 0.75$ and $G = 0.14$. The units for r are inverse of time; the scale for r is arbitrary for convenience.

grown to a certain size (28) or that they trigger an immune or hematological response (17, 24, 35), r may rise slowly to a maximum and finally decrease slowly. Unrelated to the theory used, when r is zero there should be no occurrence of DCS, and as r increases so should the DCS incidence (34).

Immediate model. The instantaneous risk (r_1), is defined as the relative difference between the tissue tension (Ptis, atm) and the absolute Pamb (atm) above a threshold (Thr) (26, 33, 34)

$$r_1 = G_1 \cdot (\text{Ptis} - \text{Pamb} - \text{Thr}) \cdot \text{Pamb}^{-1} \qquad (5)$$

where Ptis refers to the sum of the tissue tensions for H_2 ($Ptis_{H_2}$, atm) and He ($Ptis_{He}$, atm) and G_1 is a scaling factor (min^{-1}) to be determined from the fitting procedure. The inclusion of a threshold parameter has been shown to improve the fit for some human data sets (33), whereas this parameter has not been very successful in describing others (26). The contributions of O_2, CO_2, and water vapor to Pamb (1) were ignored, as in some other DCS modeling efforts (29). In this model, r_1 is constrained to be ≥ 0, and, accordingly, r_1 will be set to 0 at any time Pamb > Ptis (33, 34). The maximum value of r_1 is reached at arrival at 11 atm, after which it decreases quickly as Ptis approaches Pamb (Fig. 1*A*).

Delayed model. The second model has the same structure as the Immediate model, but here the relative supersaturation is integrated over the exposure time (34)

$$r_2 = G_2 \cdot \int_0^T (\text{Ptis} - \text{Pamb} - \text{Thr}) \cdot \text{Pamb}^{-1}\, dt \qquad (6)$$

For this model, the relative supersaturation is integrated from the first occurrence that Ptis > Pamb, followed by integration of both positive and negative values of supersaturation. However, the risk cannot be negative, so r_2 is constrained to be ≥ 0. The value of r_2 increases more slowly compared with r_1 and reaches its maximum value at the time when Pamb > Ptis (Fig. 1*B*). As can be seen in Fig. 1*C*, the r_2 maximum value occurs slightly later in the decompression compared with r_1. This leads to a delayed effect on the accumulation of P(DCS) for the Delayed model (Fig. 1*B*) compared with the Immediate model (Fig. 1*A*).

Tissue Inert Gas Tension

A single exponential gas kinetics model was used to describe the tissue tensions of the inert gases, assuming a single compartment. In other words, the animal was considered to be composed of a single tissue, with a single perfusion rate and tissue gas solubility. A more complex model is often used to describe real tissues, in which the diver is assumed to be composed of several tissues with varying perfusion rates and gas solubilities (15). For this study, the models assumed that the gas uptake and elimination followed symmetrical exponential kinetics (34).

The differential equation used to describe the inert gas tissue tension was as follows

$$\frac{d\text{Ptis}}{dt} = \frac{\text{Pblood}}{\tau} - \frac{\text{Ptis}}{\tau} \qquad (7)$$

where Ptis is the tissue tension of the inert gas (atm), Pblood is the arterial blood tension of the inert gas (atm), τ is the time constant (min) to be determined from the data, and t is time (min). The time constant determines the flux of gases in and out of the tissues. The change in Pblood during compression and decompression is assumed to be instantaneous and therefore equal to the alveolar partial pressure for that inert gas at all times. The alveolar partial pressure in turn is assumed to be equal to the Pamb for that gas.

The effect of a change in Pblood on the Ptis is computationally extensive and has been described in detail elsewhere (26, 33). The inert gas flux during the hyperbaric experiment was calculated by dividing the compression and decompression sequence into pressure-time ramps (33, 34). For the present model, it is assumed that τ is the same for He and H_2. Hence, three parameters need to be determined: τ, G, and Thr.

Effect of Microbial H_2 Metabolism on $Ptis_{H_2}$

Animals injected with a H_2-metabolizing microbe, *M. smithii*, into the intestines had a significantly lower incidence of DCS compared with control animals (10, 11, 17, 18). It has also been shown that pigs have a native intestinal flora of H_2-metabolizing microbes that, if sufficiently active, provides some protection against DCS (11). It is unclear how the reduction of H_2 in the cecum and large intestine affects the presence of H_2 elsewhere in the body. Figure 2 shows the current working hypothesis on how the conversion of H_2 into H_2O and CH_4 in the intestine (*Eq. 1*) creates a sink that ultimately reduces the arterial ($Pblood_{H_2}$) and tissue tension ($Ptis_{H_2}$) throughout the body. The uptake or removal of H_2 in the various regions of the body is dependent on the local perfusion rate and the difference in the arterial and tissue tensions of H_2. Therefore, the equation used to describe the H_2 tissue tension including H_2-metabolism was as follows

$$\frac{d\text{Ptis}_{H_2}}{dt} = \frac{\text{Pblood}_{H_2} - \text{BUG}*A}{\tau} - \frac{\text{Ptis}_{H_2}}{\tau} \qquad (8)$$

where BUG is the rate of H_2 removal as determined by either the measured CH_4 release rate ($\dot{V}_{CH_4}$, mmol CH_4/min) or by the total microbial activity injected into the intestines (Inj, mmol CH_4/min). The $A_{\dot{V}_{CH_4}}$ and A_{Inj} [atm·min·(mmol CH_4)$^{-1}$] are the respective parameters to be determined. This equation assumes that the microbial metabolism of H_2 is constant throughout the hyperbaric exposure. This simplification appears justified, because our data during 3 h at constant pressure did not show any temporal changes in the metabolism of H_2 (18). Consequently, the removal of H_2 by microbial metabolism in addition to normal gas kinetics results in up to four parameters that need to be determined for each model: τ, G, Thr, and $A_{\dot{V}_{CH_4}}$ or A_{Inj}.

The parameters were determined from the data by fitting the estimated P(DCS) to the actual outcome for each hyperbaric exposure, using *Eq. 2* or *4*. If the animal did not suffer from DCS by the end of the 1-h postdecompression observation period (Tend), the hyperbaric exposure was considered to be safe throughout the experiment.

Null Models

A special case of the risk function model is a more general and simplified model in which there are no explanatory variables. This model, referred to as Null, or Constant Hazard, considers the risk to be constant (c) at all times. For both the Immediate and Delayed models before decompression begins

$$r = 0 \qquad (9A)$$

and after decompression begins

$$r = c \qquad (9B)$$

The scaling factor G is set to 1 and not considered a parameter.

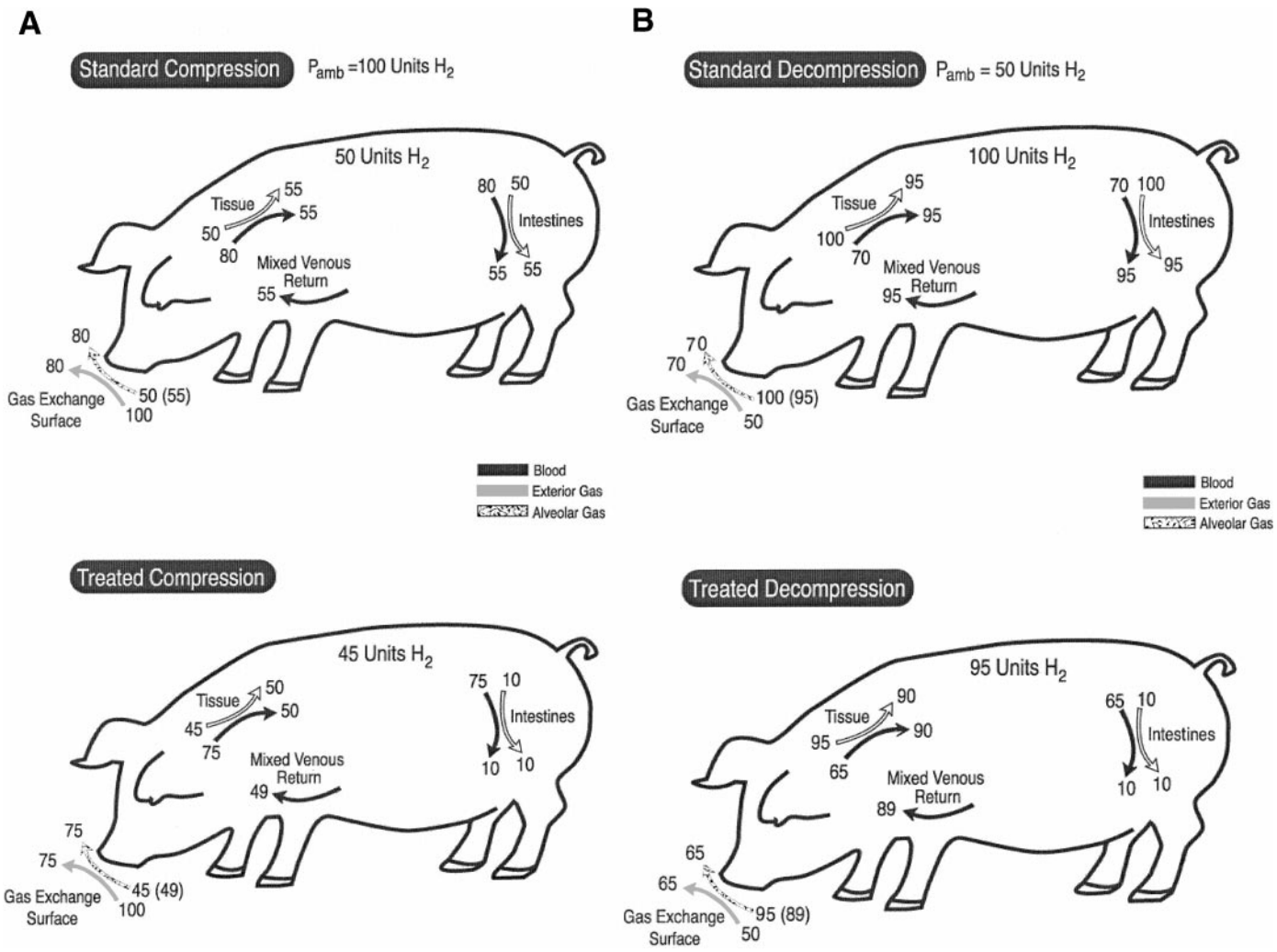

Fig. 2. Proposed physiological mechanism for H_2 biochemical decompression. For each figure, the number in parentheses represents the net result of the process of gas uptake (compression) or elimination (decompression) by the body at the end of a circulatory pass from the gas exchange surface throughout the body and returning to the gas exchange surface. Units in these figures are hypothetical and are used only to describe the current working hypothesis.

During compression (*A*, *top*) in an untreated animal exposed to a hyperbaric environment of 100 units of H_2 pressure (P_{H_2}), arterial blood is loaded with H_2 at the gas exchange surface. Alveolar P_{H_2} is somewhat less than the ambient P_{H_2}, until the tissues have reached saturation. The P_{H_2} of alveolar gas is determined by a balance of 2 processes: removal of H_2 by capillary blood to the tissues and replenishment by alveolar ventilation. By the time blood leaves the lungs, alveolar P_{H_2} is in complete equilibrium with the blood (Pblood). H_2 is delivered to all regions of the body via the arterial blood supply. H_2 in the blood diffuses into tissues until the blood and tissues are in equilibrium. Saturation is reached when Pblood, Ptis, and Pamb are all equal.

In the treated animal (*A, bottom*), the process is slightly different. Microbial metabolism of H_2 in the intestines works as a sink, resulting in a mixed venous return that will have a lower P_{H_2} compared with the untreated animal. As venous blood reaches the lung, alveolar P_{H_2} will be somewhat lower than in the untreated animal, assuming that the ventilation is the same in the treated and untreated animal. The result is a slightly lower arterial P_{H_2} compared with the untreated animal. Overall magnitude is dependent on the efficacy of the metabolism of H_2. The result is a prolonged time to equilibrium, a somewhat lower $Ptis_{H_2}$ at equilibrium, and a chronically subsaturated state.

During decompression (*B*, *top*), fluxes of inert gases are reversed. In the case of the untreated animal, H_2 is transported from tissues to blood and via the blood to the gas exchange surface. This leads to a continuous decrease in the $Ptis_{H_2}$. In a treated animal, there is a dual removal of H_2: one from the intestines and one from the gas exchange surface. This enhances the reduction of the $Ptis_{H_2}$ in the treated animal. The lower overall $Ptis_{H_2}$ of the mixed venous blood in the treated animal (*B*, *bottom*) may result in a lower risk of bubble formation compared with the untreated animal, thereby reducing the probability of DCS.

Model Analysis

A Marquardt nonlinear parameter estimation routine using maximum likelihood was used to search for best fitting parameters (31). The likelihood ratio test was used to determine significance of parameters compared with the Null models (31) and between nested models (7). In this test, significance is defined by increases in the log-likelihood (LL) values of the models (i.e., significantly smaller negative LL values). A grid search over all floating parameters, involving over 500 unique starting parameter-value sets, was used to increase the likelihood of finding global rather than local LL

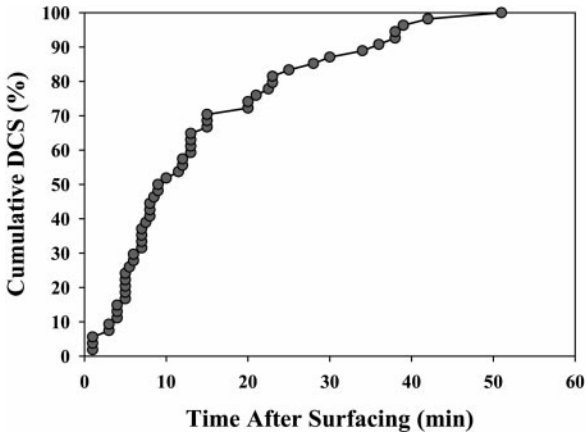

Fig. 3. Cumulative number of DCS cases with time after observation pressure (11 atm) is reached for the 53 observed cases of DCS out of 109 hyperbaric H_2 exposures.

maxima. Differences were considered significant at the $P < 0.05$ level.

RESULTS

The cumulative distribution of the 53 cases of DCS vs. time is shown in Fig. 3. The data show that the occurrence of DCS was tightly clustered within the first half hour after reaching the observation pressure (11 atm, Fig. 3). No cases of DCS were observed during the transition to lower chamber pressure (Fig. 3).

The results for the Immediate (*Eqs. 4* and *5*) and Delayed (*Eqs. 4* and *6*) models are summarized in Table 2. Each model was tested with varying numbers and combinations of the model parameters (Imm 1–4 for the Immediate model and Del 1–6 for the Delayed model). Both models showed improvement compared with the Null model (Table 2, Null vs. Imm1 and Null vs. Del1). Therefore, incorporating a specific description of the dive history significantly improved the fit to the data. The LL values cannot be used to compare the Immediate and Delayed models with each other because neither is a subset of the other.

Addition of the threshold parameter Thr to the risk function improved the fit only for the Delayed model (Table 2, Del2, and Del5). The standard errors of the Thr parameter estimates were nearly equal to or greater than the parameter estimates themselves (Table 2). Likelihood ratio analysis of this determined that the 95% confidence limit, as based on change in the LL by 1.95 units, was asymmetric about the Thr parameter (data not shown).

Inclusion of the parameter for H_2 metabolic activity injected into the animals (A_{Inj}) improved the fit for both the Immediate and Delayed models (Table 2, Imm3, Del3, and Del5). The parameter for CH_4 release rate ($A_{\dot{V}CH_4}$) improved the fit only for the Delayed model (Table 2, Del4). Only the Delayed model could successfully be fitted using four parameters, including both Thr and A_{Inj} as best fit parameters (Table 2, Del5). There was a trend for an improvement in fit when both $A_{\dot{V}CH_4}$ and Thr were included in the Delayed model ($P < 0.10$, Table 2, Del6). Activity injected and $\dot{V}CH_4$ were significantly correlated with each other ($r = 0.60$, $P < 0.001$; Fig. 4); thus no model was tested that included both A_{Inj} and $A_{\dot{V}CH_4}$.

The observed vs. predicted DCS incidences for both models were tested by separating the data into groups divided by treatment or by varying compression and decompression sequences (Fig. 5). The Immediate (Imm3) and Delayed (Del4 and Del5) models satisfactorily predicted the number of DCS cases when the data set was divided into two groups (all controls vs. all treated, χ^2 test, $P > 0.4$–0.8; Fig. 5*A*), four groups (controls at 3 different decompression rates vs. all treated animals, $P > 0.3$–0.7; Fig. 5*B*), or 14 different groups (controls vs. treated using all dive sequences listed in Table 1, $P > 0.2$–0.7; Fig. 5*C*). There was no apparent advantage to any one of these models over the other two (Fig. 5).

DISCUSSION

DCS is notoriously difficult to diagnose because its manifestations are so varied and nonspecific (16).

Table 2. *Parameter estimates and LL for Imm and Del models for the whole data set*

Model	τ, min	G, min^{-1}	Thr, atm	$A_{\dot{V}CH_4}$, atm·min·(mmol CH_4)$^{-1}$	A_{Inj}, atm·min·mmol CH_4^{-1}	LL	P
Null		0.010				−122.36	
Imm1	0.80 ± 0.13	2.23 ± 0.74				−68.90	<0.01
Imm2	1.72 ± 2.09	1.15 ± 1.28	0.35 ± 0.76			−68.34	>0.1
Imm3	0.76 ± 0.11	2.90 ± 0.96			0.18 ± 0.05	−65.58	<0.01
Imm4	0.85 ± 0.16	2.33 ± 0.78		0.94 ± 0.74		−67.99	>0.1
Del1	0.75 ± 0.06	0.14 ± 0.03				−90.58	<0.01
Del2	1.91 ± 1.18	0.08 ± 0.04	0.47 ± 0.44			−79.99	<0.01
Del3	0.74 ± 0.06	0.21 ± 0.06			0.16 ± 0.04	−80.35	<0.01
Del4	0.86 ± 0.08	0.17 ± 0.04		1.24 ± 0.38		−84.03	<0.01
Del5	1.73 ± 0.99	0.12 ± 0.06	0.40 ± 0.39		0.33 ± 0.18	−72.91	<0.01
Del6	1.75 ± 1.01	0.10 ± 0.05	0.36 ± 0.38	1.32 ± 0.96		−78.32	<0.1

Values are means ± SE ($n = 109$). LL, log-likelihood; Imm, immediate models; Del, delayed models. Model test results are shown for additions of the various test parameters (Imm1–Imm4 and Del1–Del6). Null corresponds to the Null (Constant Hazard) model; τ, time constant; G, scale factor; Thr, threshold factor; $A_{\dot{V}CH_4}$, scale factor for the CH_4 release rate, and A_{Inj}, scale factor for the total H_2-metabolizing activity injected. The P value is based on LL ratio testing between nested models (7). G units for Del models are mm^{-2}.

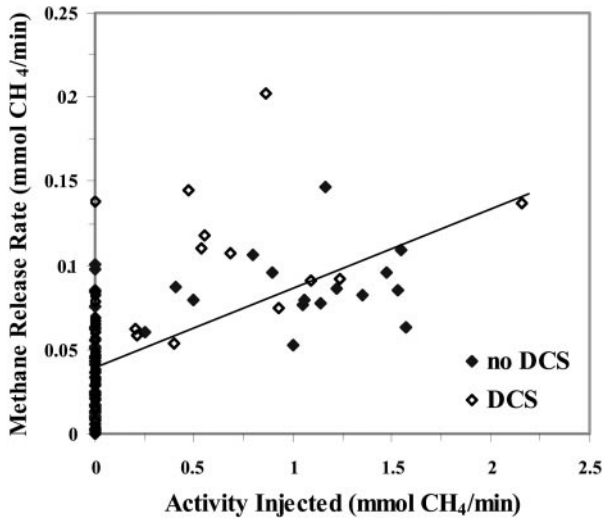

Fig. 4. Rate of release of CH_4 from animals vs. microbial activity injected into animals. Line represents least squares linear regression ($y = 41.2 + 0.048x$; $r = 0.60$, $P < 0.0001$). DCS outcome is indicated for each animal.

Choosing compression and decompression sequences with severe and rapid-onset outcomes as in this study helps reduce the subjectivity of the diagnosis. In this study, most DCS cases were unambiguous seizures or limb paralysis that occurred within the first 20 min after arrival at the lower chamber pressure (Fig. 3). This is similar to other studies on DCS in pigs (9), sheep (2), and rats (20). Previous experience with a pig model has indicated that virtually all manifestations of severe DCS will be evident within 1 h, with observation periods of 4–24 h adding more cases in less than 1% of tested animals (9). In a sheep model of DCS (2), a small number of cases continued to be diagnosed in the second and third hour of observation, but these may have been less severe symptoms. In DCS research in humans, symptoms may emerge as late as 20 h after return to 1 atm (2, 34). The prolonged latency observed in humans but not found in other animals may be an experimental artifact, because only obvious and early signs of DCS can be evaluated in other animals. Furthermore, other animals have only limited ability to report symptoms. Postdecompression, most pigs in this study manifested livid marks on the skin that are typical of skin DCS (6). We cataloged these marks for future reference but did not consider them sufficient to diagnose a case of DCS. This is in keeping with the practice for human divers of not offering recompression treatment for such mild symptoms alone.

Probabilistic models for DCS have been used successfully to model human and sheep data (2, 22, 26, 31, 33, 34). The fitted values were made from the observed outcome and the physical history of the hyperbaric experiment. Physiological interpretation of the parameters from these past studies must be made with care, because no actual physiological measurements were included. In contrast, in this study the proposed mechanism of biochemical decompression has been incorporated into the models. This mechanism is described in detail in Fig. 2. We were able to include in the models a measured physiological variable that is subject to manipulation, namely an estimate of the rate at which intestinal microbes were eliminating a portion of the

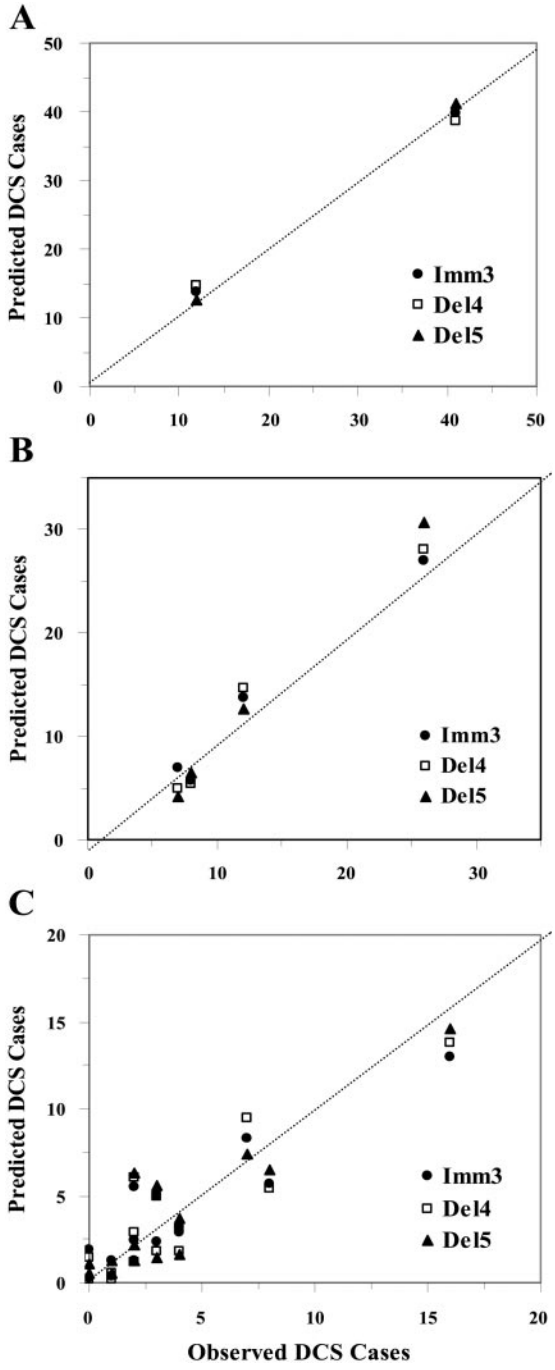

Fig. 5. Observed number of cases of DCS vs. number of cases predicted by the Immediate (Imm3) and Delayed (Del4 and Del5) models. *A*: data divided into control and treated animal groups only. *B*: data divided into all treated animals and controls at either 0.45, 0.90, or 1.8 atm/min decompression rate. *C*: data divided into all 14 of the control and treated animal groups at all compression and decompression sequences used. Dotted line in each panel has a slope of unity, representing perfect fit of predictions to observations. All 3 models could satisfactorily predict DCS incidence values that were not different from the observed values, regardless of the manner of assigning groups ($P > 0.20$).

body burden of H_2. The inclusion of such a variable will permit an evaluation of the beneficial effects of H_2 biochemical decompression in pigs from any compression and decompression sequence in H_2 and will be one of the first demonstrations of a mathematical model using a measured physiological variable to predict DCS.

Various models were tested and not found to have better fitting ability or any additional insights compared with those reported here. Among these were models with more than one tissue, models with a separate τ for H_2 and He, models with a separate τ during compression and decompression, models with a T_1 set by the observers at 11 atm, and models incorporating body weight and chamber temperature.

The successful incorporation of a parameter for H_2 metabolism in the models supports our hypothesis (19) that the H_2-metabolizing microbes reduced P(DCS) by causing an overall reduction in $Pblood_{H_2}$ (*Eq. 8*). Two terms for H_2 metabolism were tested (Table 2): one relating the removal of H_2 in the pigs' tissues to the in vitro measurement of the total activity of H_2-metabolizing microbes injected into the intestines of the animals (A_{Inj}) and the other relating the removal of H_2 to the measured CH_4 release rate ($A_{\dot{V}CH_4}$) from the pigs. These two estimates of microbial H_2 elimination were significantly correlated with each other (Fig. 4), with $\dot{V}CH_4$ ~10% of Inj (range 4–30%).

Inclusion of the parameter A_{Inj}, along with τ and G, improved the fit to the data for both the Immediate and Delayed models, compared with models with only two parameters (τ and G, Table 2, Imm1 and Del1). The parameter $A_{\dot{V}CH_4}$, on the other hand, improved the fit only for the Delayed model. Using $\dot{V}CH_4$ had lower predictive power than using Inj in the Delayed model (Table 2, compare LL values for Del3 vs. Del4 and Del5 vs. Del6). This probably indicates a greater accuracy in measuring the metabolic activity of the microbes in vitro before their injection compared with measuring the release of CH_4 into the chamber by the animals (18). In the latter case, multiple steps separate the evolution of a CH_4 molecule inside the animal from sampling it by the gas chromatograph, with unknown kinetics and sampling errors at each of these steps. Accurately estimating the $\dot{V}CH_4$ during the hyperbaric experiment is complicated by the large volumes of chamber gas (chamber gas volume at 24 atm is equivalent to 135,000 liters at 1 atm) and the necessarily slow exhaust rate of the chamber (18). Furthermore, the metabolism of H_2 within the intestinal ecosystem is more complex than the metabolic pathway shown in *Eq. 1*. Although methanogenesis is the predominant pathway for microbial H_2 metabolism (21, 25), reduction of sulfate and nitrate and formation of acetate may also consume H_2 (13, 21, 25). The potential that not all H_2 metabolism was due to methanogenesis by *M. smithii* may mask part of the correlation between $\dot{V}CH_4$ and DCS outcome (Table 2; Fig. 4).

The total H_2 tissue burden eliminated by the intestinal H_2-metabolizing microbes is a crucial link between the $Ptis_{H_2}$ and the DCS risk. The model (Del5) provides us with a way to assess the fraction of dissolved H_2 (Ptis; that is, $Ptis_{H_2}$ + $Ptis_{He}$) removed by means of microbial metabolism. For this calculation, a treated animal compressed to 24 atm for 3 h and decompressed at 0.90 atm/min will be used (Table 1). By using the parameter for A_{Inj}, the difference in Ptis for an animal with or without intestinal injections of *M. smithii* can be estimated. Let us consider an animal with an Inj of 1.50 mmol CH_4/min (activity injection in the upper range of those used in the study; Fig. 4). The estimated Ptis from this computation was compared with an animal with an Inj = 0 mmol CH_4/min. On the basis of the model computations, it can be shown that the fraction of the total gas burden removed with additional injections of *M. smithii* is ~5%. In a previous study of H_2 biochemical decompression in rats, there was a 50% reduction in DCS incidence associated with an elimination by the intestinal H_2-metabolizing microbes of ~5% of the estimated total gas burden (19). The calculation in rats depended on numerous assumptions and simplifications regarding H_2 solubility in tissues. The calculation performed above for pigs used fewer assumptions but arrived at a similar numerical result. Calculations based on H_2 solubility in pigs have generated results that are on the order of 2–19% reduction of total gas burden for similar decreases in DCS incidence (18).

A graphical example of the possible reduction in the Ptis using Inj and Thr with and without a high dose of H_2-metabolizing microbes is shown in Fig. 6. Because risk of DCS is the area under the curve between Ptis and Pamb, where Ptis > Pamb, the beneficial effects of biochemical decompression can be seen (Fig. 6). Even though the two curves for Ptis for control and treated animals are close, the difference in the area under the curve between Ptis and Pamb is appreciable for DCS risk [Fig. 6, compare $P(DCS)_C$ vs. $P(DCS)_T$]. This illus-

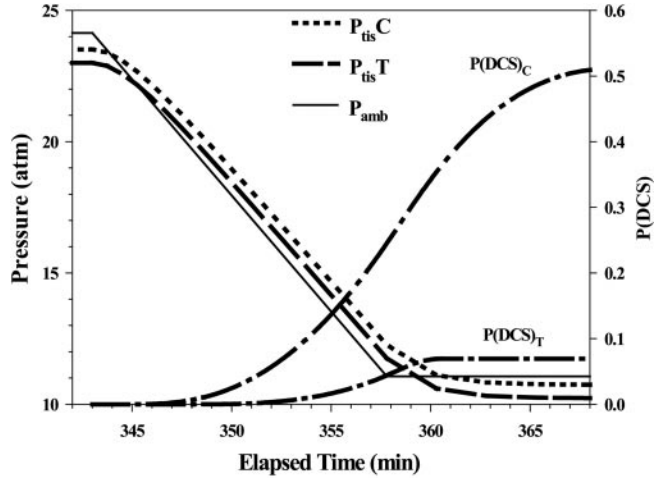

Fig. 6. Ambient pressure (Pamb) and tissue tension of H_2 + He for a control animal (PtisC) and a treated animal (PtisT) injected with a total H_2-metabolizing activity of 1.50 mmol CH_4/min and the estimated probability of DCS for a control [$P(DCS)_C$] and treated animal [$P(DCS)_T$] using the 4-parameter Delayed model (Table 2, Del5). Hyperbaric exposure was to a total pressure of 24 atm for 3 h with a decompression rate of 0.9 atm/min.

trates how elimination of relatively small fractions of dissolved gas may have a surprisingly large impact on the DCS incidence.

The models described here can be used to predict the overall benefit from H_2 biochemical decompression for any specified compression and decompression sequence. On the basis of the parameter estimates, it is possible to predict the change in the P(DCS) with varying $\dot{V}_{CH_4}$ or Inj for any given hyperbaric sequence. For example, the most tested compression and decompression sequence in this study was to a total pressure of 24 atm for 3 h with a decompression rate of 0.9 atm/min ($n = 20$ control and 18 treated animals, Table 1). The observed DCS incidence was 80% (16 cases) and 39% (7 cases) for control and treated animals, respectively (Table 1). The predicted values for the Delayed (Del5) model with inclusion of Inj and Thr were 73% (14.6 cases) and 41% (7.4 cases) for control and treated animals, respectively (Fig. 5*C*). The reduction in DCS risk predicted by the Delayed model with inclusion of Inj is thus close to the observed value. The Imm3 and Del4 model predictions were only 1–2 DCS cases different from the Del5 model predictions (Fig. 5*C*). Naturally, predictions of P(DCS) made for dive exposures or treatment dosages beyond our data set must be made with caution and tested empirically before the full benefit of this model can be evaluated.

In conclusion, a hypothesis of the mechanism supporting biochemical decompression (Fig. 2) has been postulated and incorporated into a physiologically based probabilistic model (*Eq. 8*). The model can be used to predict the beneficial effects of biochemical decompression from any compression and decompression sequence with pigs in hyperbaric H_2. The physiological interpretation of the model gives a foundation for further research including other physiological measurements related to gas transport kinetics and estimates of tissue inert gas content. The model supports our hypothesis that removal of H_2 by microbial metabolism reduces the body burden of gas, thereby reducing the DCS risk by as much as 50%.

We gratefully thank Diana Temple for editorial assistance and critical reading of this manuscript. We also thank A. Mulligan for graphical help with Fig. 2. We are grateful for the comments by the anonymous referees that we believe helped improve the readability of the paper. Also, we would like to thank C. McClure, H. Hung, and S. Maritz for sharing statistical expertise.

This work was funded by the Naval Medical Research and Development Command Work Unit no. 61153N MR04101.00D-1103. The opinions and assertions contained herein are the private ones of the authors and are not to be construed as official or reflecting the views of the Navy Department and the naval service at large.

Data were taken from animal experiments previously reviewed and approved by the Institutional Animal Care and Use Committee according to the principles set forth in the *Guide for the Care and Use of Laboratory Animals,* Institute of Laboratory Animal Resources, National Research Council, National Academy Press, 1996.

REFERENCES

1. **Antonisen NR and Fleetham JM.** Ventilation: total, alveolar, and dead space. In: *Handbook of Physiology. The Respiratory System. Gas Exchange*. Bethesda, MD: Am. Physiol. Soc., 1987, sect. 3, vol. IV, chapt. 7, p. 113–129.
2. **Ball R, Lehner CE, and Parker EC.** Predicting risk of decompression sickness in humans from outcomes in sheep. *J Appl Physiol* 86: 1920–1929, 1999.
3. **Broome JR and Dick EJ Jr.** Neurological decompression illness in swine. *Aviat Space Environ Med* 67: 207–213, 1996.
4. **Broome JR, Dutka AJ, and McNamee GA.** Exercise conditioning reduces the risk of neurologic decompression illness in swine. *Undersea Hyperb Med* 22: 73–85, 1995.
5. **Broome JR, Pearson RR, and Dutka AJ.** Failure to prevent decompression illness in rats by pretreatment with a soluble complement receptor. *Undersea Hyperb Med* 21: 287–295, 1994.
6. **Buttolph TB, Dick EJ Jr, Toner CB, Broome JR, Williams R, Kang YH, and Wilt NL.** Cutaneous lesions in swine after decompression: histopathology and ultrastructure. *Undersea Hyperb Med* 25: 115–121, 1998.
7. **Collett D.** *Modelling Survival Data in Medical Research*. London, UK: Chapman & Hall, 1994.
8. **Cross S, Jennings K, and Thomson L.** Decompression sickness: role of patent foramen ovale is limited. *BMJ* 309:743–744, 1994.
9. **Dromsky D, Toner CB, Survanshi S, Fahlman A, Parker E, and Weathersby P.** The natural history of severe decompression sickness after rapid ascent from air saturation in a porcine model. *J Appl Physiol* 89: 791–798, 2000.
10. **Fahlman A, Kayar SR, Becker WJ, Lin WC, and Whitman WB.** Decompression sickness risk correlated with activity of H_2-metabolizing microbes injected in pigs prior to dives in H_2. *Undersea Hyperb Med* 26: 20, 1999.
11. **Fahlman A.** *On the Physiology of Hydrogen Diving and Its Implication for Hydrogen Biochemical Decompression* (PhD thesis). Ottawa, Ontario, Canada: Carleton University, 2000.
12. **Germonpré P, Dendale P, Unger P, and Balestra C.** Patent foramen ovale and decompression sickness in sports divers. *J Appl Physiol* 84: 1622–1626, 1998.
13. **Gibson GR, Cummings JH, and Macfarlane GT.** Competition for hydrogen between sulphate-reducing bacteria and methanogenic bacteria from the human large intestine. *J Appl Bacteriol* 65: 241–247, 1988.
14. **Hills BA.** *Decompression Sickness*. New York: Wiley, 1977.
15. **Homer LD, Weathersby PK, and Survanshi S.** How countercurrent blood flow and uneven perfusion affect the motion of inert gas. *J Appl Physiol* 69: 162–170, 1990.
16. **Jain KK.** *Textbook of Hyperbaric Medicine*. Toronto, Ontario, Canada: Hogrefe & Huber, 1990.
17. **Kayar SR, Aukhert EO, Axley MJ, Homer LD, and Harabin AL.** Lower decompression sickness risk in rats by intravenous injection of foreign protein. *Undersea Hyperb Med* 24: 329–335, 1997.
18. **Kayar SR, Fahlman A, Lin WC, and Whitman WB.** Increasing activity of H_2-metabolizing microbes lowers decompression sickness risk in pigs during H_2 dives. *J Appl Physiol* 91: 2713–2719, 2001.
19. **Kayar SR, Miller TL, Wolin MJ, Aukhert EO, Axley MJ, and Kiesow LA.** Decompression sickness risk in rats by microbial removal of dissolved gas. *Am J Physiol Regulatory Integrative Comp Physiol* 275: R677–R682, 1998.
20. **Lillo RS, Parker EC, and Porter WR.** Decompression comparison of helium and hydrogen in rats. *J Appl Physiol* 82: 892–901, 1997.
21. **Miller TL.** Biogenic sources of methane. In: *Microbial Production and Consumption of Greenhouse Gases: Methane, Nitrogen Oxides, and Halomethanes*, edited by Rogers JE and Whitman WB. Washington, DC: Am. Soc. Microbiol., 1991, p. 175–187.
22. **Parker EC, Survanshi SS, Massell PB, and Weathersby PK.** Probabilistic models of the role of oxygen in human decompression sickness. *J Appl Physiol* 84: 1096–1102, 1998.
23. **Robertson AG.** Decompression sickness risk in women (letter). *Undersea Biomed Res* 19: 216–217, 1992.
24. **Stevens DM, Gartner SL, Pearson RR, Flynn ET, Mink RB, Robinson DH, and Dutka AJ.** Complement activation during saturation diving. *Undersea Hyperb Med* 20: 279–288, 1993.
25. **Strocchi AJ, Furne K, Ellis CJ, and Levitt MD.** Competition for hydrogen by human faecal bacteria: evidence for the predominance of methane producing bacteria. *Gut* 32: 1498–1501, 1991.

26. **Thalmann ED, Parker EC, Survanshi SS, and Weathersby PK.** Improved probabilistic decompression model risk predictions using linear-exponential kinetics. *Undersea Hyperb Med* 24: 255–274, 1997.
27. **Van Liew HD and Hlastala MP.** Influence of bubble size and blood perfusion on absorption of gas bubbles in tissues. *Respir Physiol* 7: 111–121, 1969.
28. **Vann RD.** Mechanisms and risks of decompression. In: *Diving Medicine*, edited by Bove AA and Davis JC. Philadelphia, PA: Saunders, 1990, p. 29–49.
29. **Weathersby PK, Hartn BL, Flynn ET, and Walker WF.** Role of oxygen in the production of human decompression sickness. *J Appl Physiol* 63: 2380–2387, 1987.
30. **Weathersby PK and Homer LD.** Solubility of inert gases in biological fluids and tissues: a review. *Undersea Biomed Res* 7: 277–296, 1980.
31. **Weathersby PK, Homer LD, and Flynn ET.** On the likelihood of decompression sickness. *J Appl Physiol* 57: 815–825, 1984.
32. **Weathersby PK, Survanshi SS, Hays JR, and MacCallum ME.** *Statistically based decompression tables III: Comparative Risk Using U. S. Navy, British, and Canadian Standard Schedules*. Bethesda, MD: Naval Medical Research Institute, 1986. (Technical Report NMRI 86-50).
33. **Weathersby PK, Survanshi SS, Homer LD, Hart BL, Nishi RY, Flynn ET, and Bradley ME.** *Statistically Based Decompression Tables I. Analysis of standard air dives: 1950–1970*. Bethesda, MD: Naval Medical Research Institute, 1985, NMRI 85-16.
34. **Weathersby PK, Survanshi SS, Homer LD, Parker E, and Thalmann ED.** Predicting the time of occurrence of decompression sickness. *J Appl Physiol* 72: 1541–1548, 1992.
35. **Zhang J, Fife CE, Currie MS, Moon RE, Piantadosi CA, and Vann RD.** Venous gas emboli and complement activation after deep repetitive air diving. *Undersea Biomed Res* 18: 293–302, 1991.